

Article

**Arrested Coalescence of Particle-coated Droplets  
into Nonspherical Supracolloidal Structures**

Andre# R. Studart, Ho Cheung Shum, and David A. Weitz

*J. Phys. Chem. B*, **2009**, 113 (12), 3914-3919 • DOI: 10.1021/jp806795c • Publication Date (Web): 07 January 2009

Downloaded from <http://pubs.acs.org> on April 13, 2009

**More About This Article**

Additional resources and features associated with this article are available within the HTML version:

- Supporting Information
- Access to high resolution figures
- Links to articles and content related to this article
- Copyright permission to reproduce figures and/or text from this article

[View the Full Text HTML](#)



**ACS Publications**  
High quality. High impact.

The Journal of Physical Chemistry B is published by the American Chemical Society, 1155 Sixteenth Street N.W., Washington, DC 20036

# Arrested Coalescence of Particle-coated Droplets into Nonspherical Supracolloidal Structures<sup>†</sup>

André R. Studart,<sup>\*,‡,§,▽</sup> Ho Cheung Shum,<sup>§</sup> and David A. Weitz<sup>‡,§</sup>

Department of Physics and School of Engineering and Applied Sciences, Harvard University, Cambridge, Massachusetts, USA.

Received: July 30, 2008; Revised Manuscript Received: November 10, 2008

Colloidal and supracolloidal structures with anisotropic shape and surface chemistry are potential building blocks for the fabrication of novel materials. Droplets or bubbles are often used as templates for the assembly of particles into supracolloidal structures of spherical shape. Particle-coated droplets or bubbles have recently been shown to also retain nonspherical geometries after deformation, suggesting that the templating approach can also be used to produce supracolloidal structures with anisotropic shape. We show that partially coated droplets generated in a microcapillary device can undergo spontaneous coalescence into stable nonspherical structures. By positioning the droplets into regular arrays before coalescence, we produce anisotropic geometries with well-defined bonding angles between adjacent merged droplets. This approach allows for the fabrication of novel anisotropic supracolloidal structures with deliberately designed shapes.

## Introduction

Colloidal and supracolloidal structures with increasing complexity have been produced to create new materials and to emulate molecular systems at experimentally accessible microscopic scales.<sup>1,2</sup> Supracolloidal structures, in particular, can be formed by self-assembling colloidal particles on the surface of larger templating droplets or bubbles in particle-stabilized foams and emulsions (Pickering emulsions).<sup>3–8</sup> This approach has been used to produce a wide variety of structures, ranging from hollow colloidosomes<sup>4–6</sup> to particle shells and surface-patterned polymeric particles.<sup>3</sup> Because droplets and bubbles tend to relax into spherical shapes to minimize surface energy, supracolloidal structures produced with these templates are usually spherical.

However, particle-coated bubbles and droplets can also retain nonspherical shape after deformation due to the ability of the outer particle shell to withstand the unequal stresses of interfaces with unequal radii of curvature.<sup>3,9</sup> Nonspherical structures have been obtained by squeezing particle-coated air bubbles and oil droplets between glass slides<sup>9</sup> and through a glass capillary<sup>10</sup> or elongating them in sheared particle-stabilized emulsions.<sup>3,11</sup> These results suggest that supracolloidal structures can also be shaped into tailored anisotropic geometries, which can potentially be used for encapsulation or as building blocks for more complex larger architectures.<sup>12</sup>

Although the remarkable ability of the outer particle armor to prevent the relaxation of bubbles or droplets to a spherical shape has been demonstrated, this phenomenon has not yet been exploited for the controlled fabrication of nonspherical structures. To generate structures with more complex geometries using emulsions as templates, control over the formation of particle-coated droplets is needed. Because of its ability to controllably generate, manipulate, and coat droplets with

particles, microfluidics can be a powerful tool for the production of supracolloidal structures with anisotropic features.

In this paper, we report on the use of a glass microcapillary device to produce monodisperse droplets partially covered with colloidal particles that then undergo spontaneous coalescence into nonspherical structures of well-defined shape. To form stable nonspherical shapes, the coalescence process is kinetically arrested due to the jamming of the colloidal particles adsorbed at the droplet surface. We investigate the conditions required to arrest the coalescence of particle-coated droplets and show how this phenomenon can be controlled to fabricate structures with unique anisotropic shapes.

## Materials and Methods

Silica particles with diameter of  $111 \pm 10$  nm (grade MP1040, 40 wt % solids aqueous suspension, Nissan Chemical Industries Ltd., Tokyo, Japan) were used to partially cover the surface of oil droplets through adsorption at the oil–water interface. Toluene (>99.5% pure, EMD Chemicals, Gibbstown, NJ, USA), hexadecyltrimethylammonium bromide (CTAB, > 99% pure, Sigma-Aldrich Co., St Louis, MO, USA), trimethylolpropane ethoxylate triacrylate (average number molecular weight  $\approx 428$  g/mol, Sigma-Aldrich Co., St Louis, MO, USA), 1,6-hexanediol diacrylate (Sigma-Aldrich Co., St Louis, MO, USA), and 2-hydroxy-2-methyl-1-phenyl-1-propanone (Darocur 1173, Ciba Specialty Chemicals Corp., Tarrytown, NY, USA) were the nonaqueous chemicals used for the preparation of emulsions. All chemicals were used as received from the manufacturers. Ultrapure water with an electrical resistance higher than 18 M $\Omega$  cm was used in all experiments (Milli-Q Synthesis System, Millipore Corp., Billerica, MA, USA).

Monodisperse oil droplets were generated using the glass microcapillary device sketched in Figure 1. In this geometry, a tapered cylindrical tube is fitted into an outer square capillary tube to enable the coaxial flow of two immiscible fluids through the device. A square tube with inner diameter of 1.1 mm and a cylindrical tube with outer diameter of 1.0 mm were used to enable easy assembly while maintaining a good alignment of

<sup>†</sup> Part of the “PGG (Pierre-Gilles de Gennes) Memorial Issue”.

\* To whom correspondence should be addressed. E-mail: studart@seas.harvard.edu; andre.studart@mat.ethz.ch.

<sup>‡</sup> Department of Physics.

<sup>§</sup> School of Engineering and Applied Sciences.

<sup>▽</sup> Current Address: Department of Materials, ETH-Zurich, Zurich, CH 8093, Switzerland.

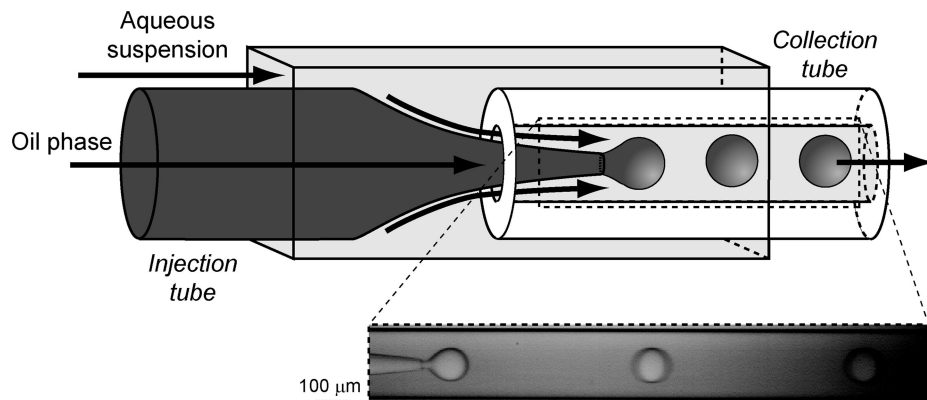


**Figure 1.** Schematic of the glass microcapillary device used for droplet formation. Inset: high-speed micrograph of monodisperse droplets generated in dripping mode.

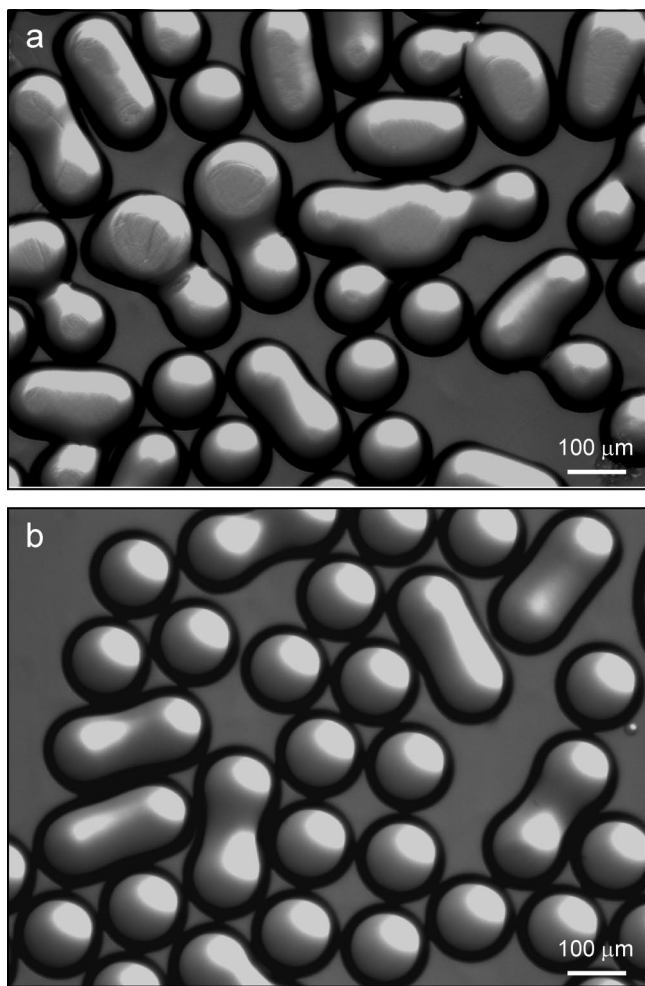


**Figure 2.** Nonspherical structures formed a few tens of seconds after deposition of single droplets on a glass substrate. These wet structures remained completely stable for several minutes before evaporation of the liquids took place. Images (a) and (b) were obtained at inner/outer flow rates of 1000/10000 and 500/5000  $\mu\text{L/h}$ , respectively, with emulsions containing 5 vol % of particles in the continuous aqueous phase.

the capillary tubes. The tapered cylindrical tube was produced by axial heating of the end of a 580  $\mu\text{m}$  inner diameter capillary tube (World Precision Instruments, Sarasota, FL, USA) using a micropipette puller (Model P-97 Flaming/Brown puller, Sutter Instrument, Novato, CA, USA).<sup>1</sup> The heating conditions were adjusted to produce tubes with an inner diameter of approximately 40  $\mu\text{m}$  at the capillary tip. To increase the speed

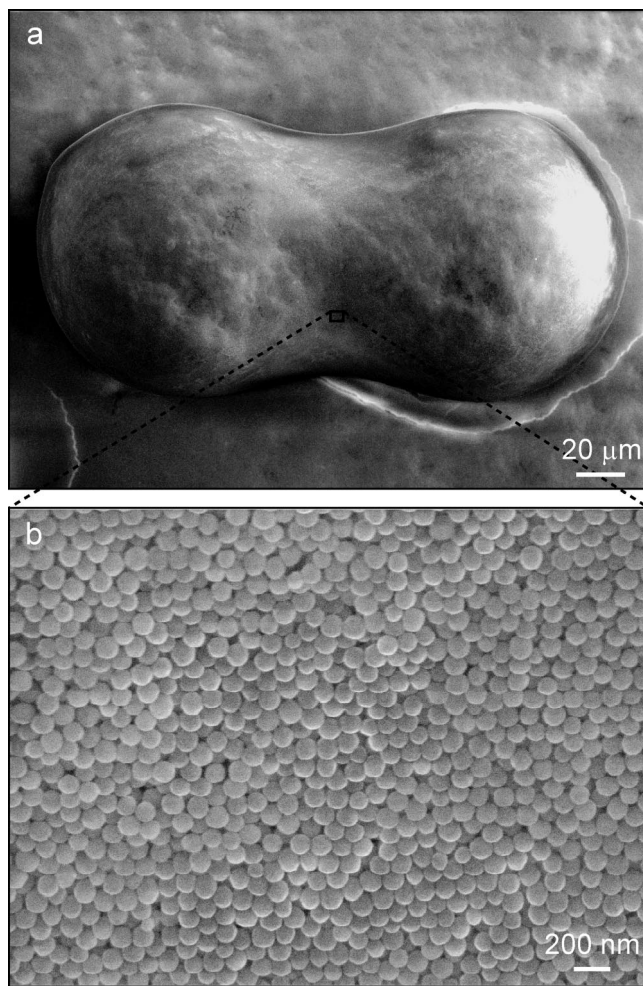


**Figure 3.** (a) Nonspherical supracolloidal structure formed by the arrested coalescence of droplets, highlighting (in b) the jammed particles in the neck region between partially coalesced droplets. The structure was obtained using an UV-polymerizable oil phase at a flow rate of 400  $\mu\text{L/h}$  as the dispersed fluid and an aqueous suspension containing 22.5 vol % of silica particles at a flow rate of 4000  $\mu\text{L/h}$  as the continuous fluid.

of the outer fluid to create smaller droplets, the tip of the tapered tube was inserted into a cylindrical collection tube with an inner diameter of 200  $\mu\text{m}$ , as shown schematically in Figure 1.

Droplets were produced in the dripping mode by pumping the oil phase through the inner cylindrical tube and an aqueous suspension of partially hydrophobic silica particles through the outer square tube, as indicated in Figure 1.



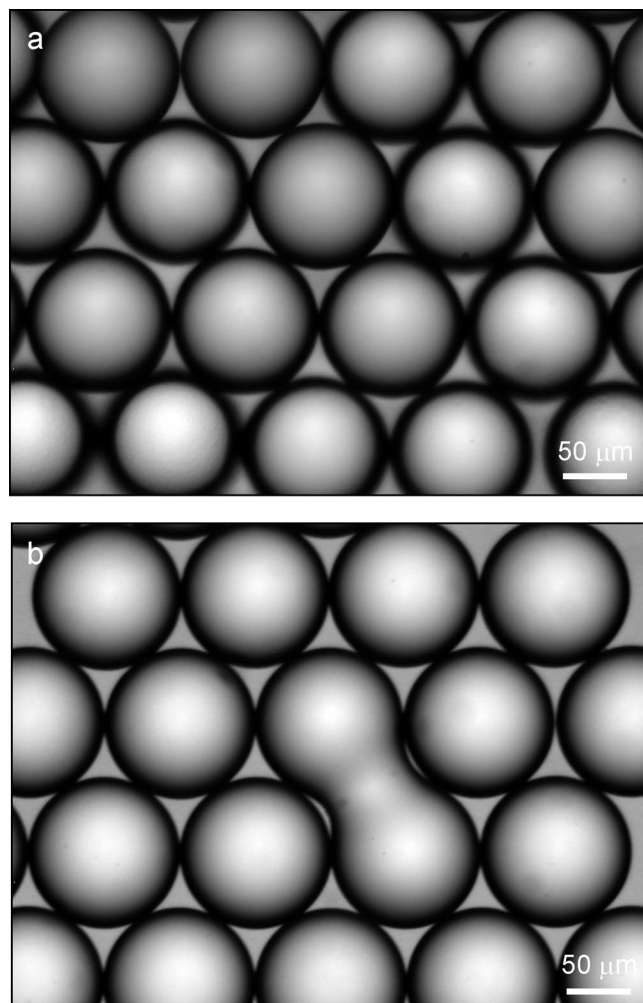


**Figure 4.** (a) Droplets self-assembled into a hexagonal array at the air–water interface before coalescence takes place. (b) Adjacent droplets previously arranged in an ordered hexagonal array forming a well-defined stable dimer after arrested coalescence.

Particles delivered through the outer aqueous phase were in situ hydrophobized to adsorb on the surface of freshly created oil droplets along the collection tube. The concentration of particles in the outer aqueous phase and the flow rates of inner and outer fluids were adjusted to control the particle coverage on the surface of droplets exiting the collection tube. The inner and outer flow rates used for droplet formation were adjusted in the ranges of, respectively, 200–1000 and 2000–15000  $\mu\text{L}/\text{min}$  using syringe pumps (Harvard apparatus, PHD 2000 Programmable, Holliston, MA, USA), whereas the concentration of silica particles in the aqueous phase was varied between 5.0 and 22.5 vol %.

Partially hydrophobic particles were generated in situ by adsorbing CTAB on the silica surface at pH 8. The hydrophobicity of the particle surface was tuned by changing the initial concentration of CTAB in the aqueous phase. An initial CTAB concentration of 0.4 mmol/L was optimum for rendering the particles sufficiently hydrophobic to adsorb at the oil–water interface, regardless of the concentration of silica particles in the aqueous phase (5.0–22.5 vol %). Lower surfactant concentrations led to unstable emulsions since particles were not hydrophobic enough to adsorb on the droplet surface. Higher CTAB concentrations resulted in very hydrophobic particles that extensively aggregated in the aqueous phase, reducing the amount of particles adsorbed at the oil–water interface. The

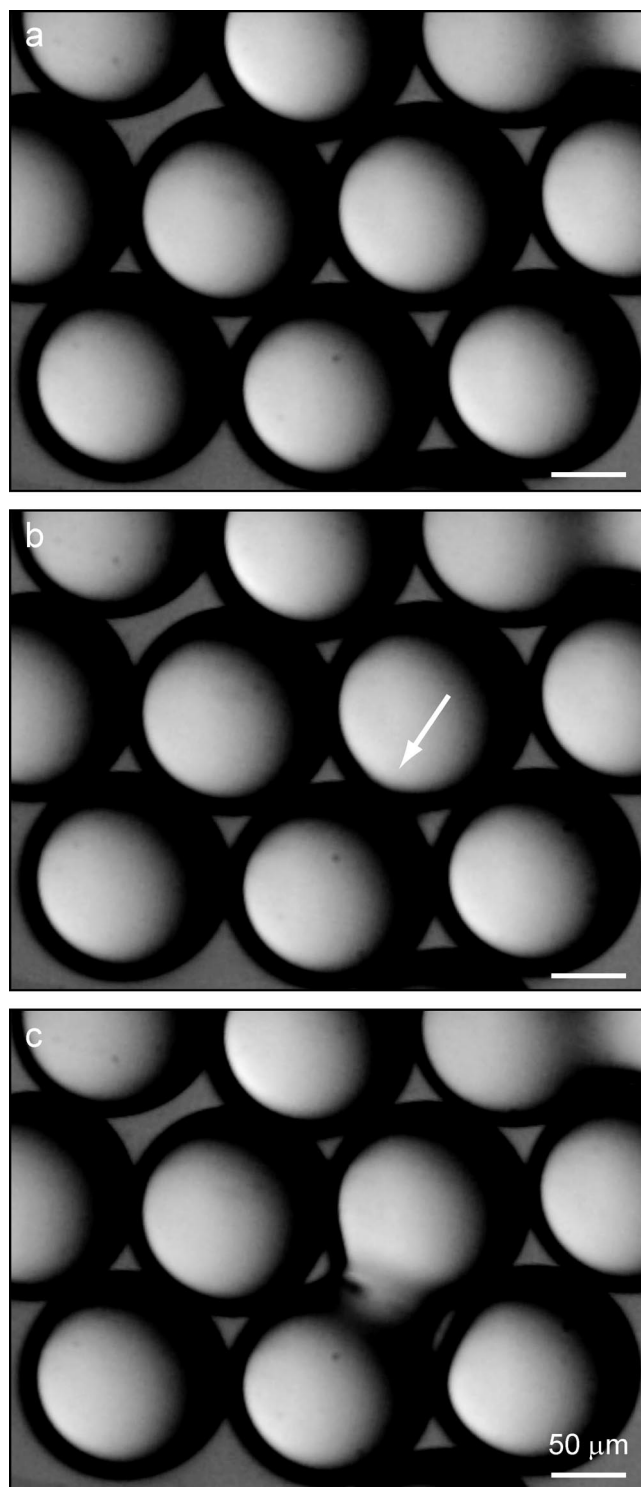


**Figure 5.** Sequence of images taken at time intervals of 50  $\mu\text{s}$  showing (a) individual droplets in a packed array, (b) the rupture of the thin liquid film between two adjacent droplets (indicated by the arrow), and (c) the partial coalescence of droplets into a nonequilibrium arrested state. Scale bars in all images correspond to 50  $\mu\text{m}$ .

optimum CTAB content of 0.4 mmol/L corresponds to 44% of the critical micelle concentration (0.9 mmol/L) and is within the range at which hemimicelles form on the silica surface to render the particles hydrophobic<sup>13–15</sup>

A high-speed camera (Vision Research, Wayne, NJ, USA) coupled to an optical microscope (model DM IRB, Leica Microsystems, Wetzlar, Germany) was used to observe droplet formation in the microcapillary device. Droplets

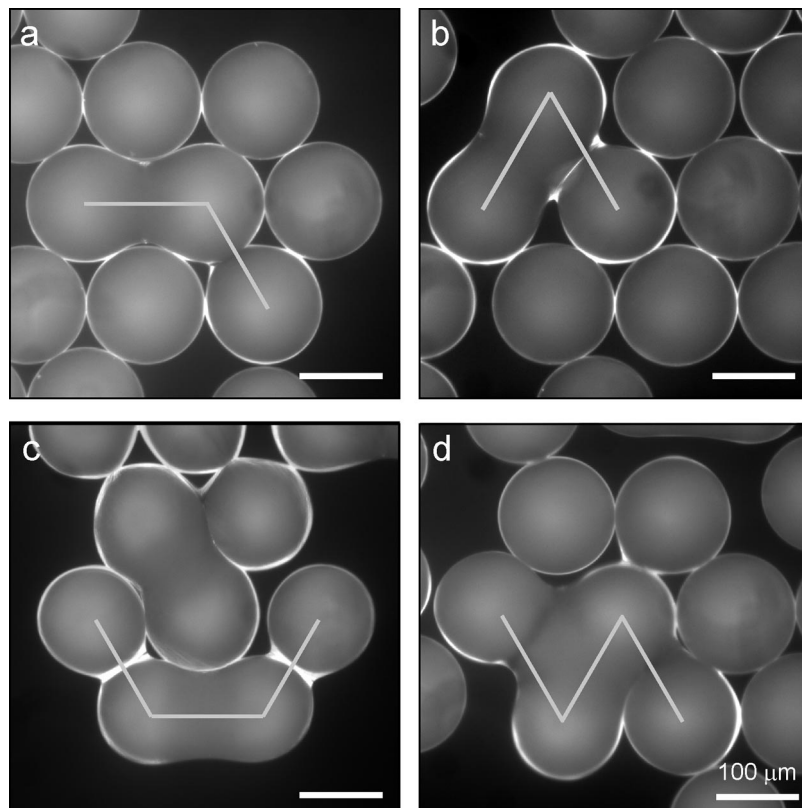


**Figure 6.** Nonspherical supracolloidal structures with complex shape obtained by positioning the oil droplets into hexagonal arrays before partial coalescence takes place. Triple structures with bonding angles of  $120^\circ$  and  $60^\circ$  are shown in images (a) and (b), respectively. Images (c) and (d) show quadruple structures with bonding angles of  $120^\circ$  in a “boat” conformation and  $60^\circ$  in a “zig-zag” conformation, respectively. Images were obtained using a polarizing filter in reflected mode with the fluorescent dye Nile Red added to the oil droplets. The gray straight lines highlight the well-defined shapes of the structures. Scale bars in all images correspond to  $100\ \mu\text{m}$ .

formed were collected on glass substrates for observation in an optical microscope under transmitted light (model DM RX, Leica Microsystems, Wetzlar, Germany). The fluorescent dye Nile Red (Sigma-Aldrich Co., St Louis, MO, USA) was added to the oil phase in some sample runs (0.03 wt % based on oil mass) to enable observation under reflected polarized light. To fix the structure of droplets and observe them with electron microscopy, a photosensitive oil mixture consisting of 45 wt % 1,6-hexanediol diacrylate (monomer), 22.5 wt % trimethylolpropane ethoxylate triacrylate (monomer), 7.5 wt % 2-hydroxy-2-methyl-1-phenyl-1-propanone (initiator), and 25 wt % toluene (diluent) was used as the oil phase during droplet formation. After collection onto a glass substrate, the oil droplets were exposed to a 325 nm ultraviolet lamp for about 3 min to polymerize the photosensitive oil mixture. Field emission scanning electron microscopy was afterward performed on Pt-coated dried samples (Supra 55VP, Carl Zeiss NTS GmbH, Oberkochen, Germany).

## Results and Discussion

Monodisperse toluene droplets with typical diameters in the range of  $100\text{--}140\ \mu\text{m}$  were generated in the microcapillary device. The concentration of toluene droplets dispersed in the aqueous suspension was varied from 5.7 to 16.7 vol % by adjusting the outer/inner flow rate ratio from 5.0 to 16.7. The emulsion was collected and spread onto a glass substrate after accumulation in the end of the cylindrical collection tube (Figure 1).

The oil droplets in the collected emulsion quickly creamed due to the lower density of toluene as compared to water. A

few seconds after collection, some of the single toluene droplets started to coalesce into larger droplets of lower surface-to-volume ratio and lower overall interfacial area. Remarkably, coalescence between these droplets was arrested before complete fusion into a larger spherical droplet, leading to the formation of stable nonspherical structures of various shapes throughout the air–water interface (Figure 2). The spherical and nonspherical structures shown in Figure 2 were completely stable for the entire time period over which the samples remained wet. Several minutes after collection on the glass substrate, the shell of particles adsorbed on the droplet surface started to buckle due to continuous evaporation of the liquid phases.

In general, coalescence was more pronounced in emulsions produced at higher flow rates and containing lower concentrations of particles in the aqueous phase. Lower particle concentrations and higher flow rates, which result in lower residence times in the collection tube, both decrease the droplet surface coverage by particles due to the lower number of particles colliding with the oil–water interface as the droplets travel along the collection tube. Droplets with a lower surface coverage exhibit larger particle-free, unprotected sites on the surface that increase the extent of coalescence, as indicated by the rounder shapes obtained at high flow rates (Figure 2a) when compared to the well-defined dumbbell geometry achieved at low flow rates (Figure 2b).

To investigate the process of arrested coalescence, we examined the surface of the nonspherical structures using electron microscopy. Nonspherical colloidosomes produced from partial fusion of single droplets exhibit dense layers of

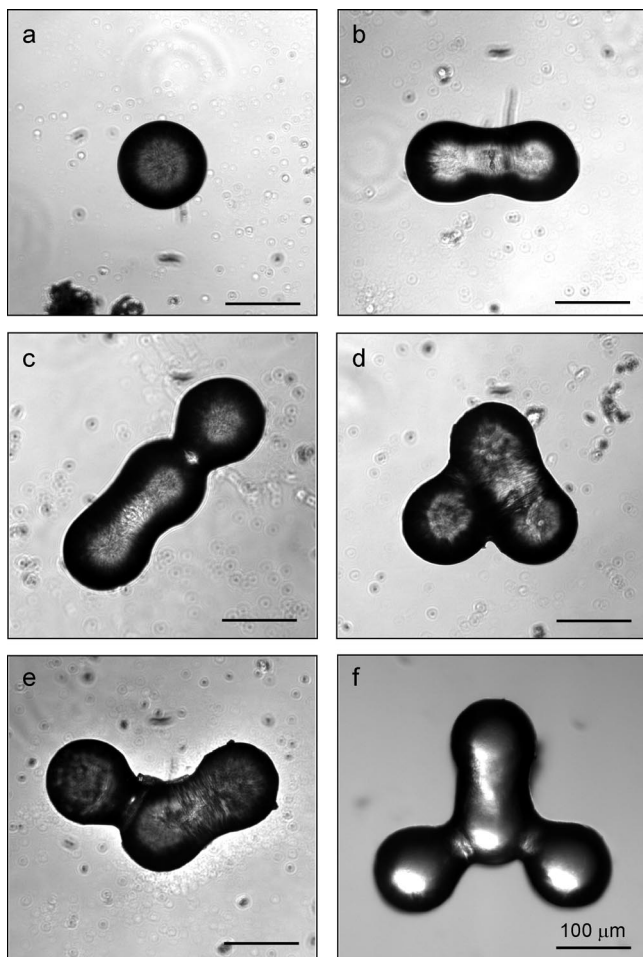


**Figure 7.** (a) Spherical and (b–f) nonspherical dried structures formed by polymerizing the inner oil phase of partially coalesced droplets. Nonspherical supracolloidal structures with bonding angles that are integers of  $60^\circ$  were obtained by arranging the individual droplets into a hexagonal array before coalescence. Scale bars in all images correspond to  $100\ \mu\text{m}$ .

jammed particles throughout the entire droplet surface (Figure 3a). Multilayers of particles are observed, particularly in the neck region, where the two droplets merge (Figure 3b). Particle jamming at the oil–water interface provides mechanical resistance against further relaxation of the droplet into a spherical shape,<sup>9</sup> ultimately arresting the coalescence process.

Assuming that particles are irreversibly adsorbed at the oil–water interface, the decrease in droplet surface-to-volume ratio during the coalescence process increases the coverage of particles on the droplet surface. For initial droplets of radii  $r_1$  and  $r_2$ , a simple geometrical analysis shows that the surface coverage after complete coalescence  $s_f$  can be described as follows:

$$s_f = (1 + \alpha^2)(1 + \alpha^3)^{-\frac{2}{3}}s_i \quad (1)$$

where  $s_i$  is the surface coverage by particles on the initial droplets before coalescence, and  $\alpha$  is the initial droplet size ratio  $r_2/r_1$ . Equation 1 predicts that complete coalescence of two identical droplets into a final spherical shape leads to an increase of 26% in the surface coverage by particles. Such an increase in surface coverage explains the jamming of particles at the oil–water interface of nonspherical structures (Figure 3).

A remarkable feature of the approach used here to produce nonspherical structures is the fact that the monodisperse droplets do not coalesce readily upon contact with each other, but instead remain as singlets for a few seconds before coalescence occurs. This enables arbitrary positioning of single droplets into a target geometry in order to generate structures with controlled nonspherical shapes after arrested coalescence. Single droplets can, for example, first self-assemble into hexagonal arrays at the air–water interface (Figure 4a) and afterward undergo arrested coalescence with an adjacent fixed droplet (Figure 4b). While self-assembly into organized arrays happens within seconds after droplet deposition, high-speed imaging revealed that the coalescence event itself happens in only a tenth of a microsecond (Figure 5 and Supporting Information).

The fact that droplets do not promptly fuse upon contact suggests that the colloidal particles adsorbed at the interface initially impede droplet coalescence. Coalescence is initiated only when particle-free patches of adjacent droplets contact each other; this may require droplet rotation or rearrangements of particles on the droplet surface to bring two particle-free regions of the interface into contact. Moreover, coalescence at one site of the droplet surface does not lead to particle jamming throughout the entire oil–water interface. As a result, particle-free patches are still present on other sites of the droplet surface, allowing each single droplet to undergo arrested coalescence with more than one adjacent droplet. It is interesting to note that droplets undergoing multiple fusion events coalesce to different extents at different merging sites, as indicated, for example, in Figure 2a. This suggests that the increase in surface coverage resulting from the first fusion process reduces the extent of coalescence at other subsequent merging sites. Such feature limits the total number of coalescence events that each merging droplet can accomplish. In general, the number of fusion sites per droplet increases for higher flow rates and lower particle concentrations in the outer aqueous phase, since these factors tend to reduce the coverage of droplets by particles and thus increase the density of particle-free patches on the droplet surface. Figure 2a shows that a maximum of three coalesced sites is observed for droplets produced at high flow rates and a low particle volume fraction.

The possibility of fixing the position of droplets into specific arrays before coalescence and the ability to induce multiple fusion events allows for the production of multiunit structures with tailored bonding angles between the merging droplets. Structures formed from droplets previously assembled in a hexagonal array for example must exhibit bonding angles that are integer multiples of  $60^\circ$ . Examples of multiunit supracolloidal structures displaying bonding angles of  $60^\circ$  and  $120^\circ$  are shown in Figure 6. Anisotropic shapes with intricate geometries can be achieved, as exemplified by the structures with zigzag and boat conformations.

These multiunit structures can be dried and harvested without impairing their well-defined structure by polymerizing the inner dispersed phase, as shown in Figure 7. Although in this study anisotropic shapes were obtained by the random coalescence of neighboring droplets, positioning droplets into templates with arbitrary configurations would enable deliberate control over the size and shape of the final structures. Moreover, supracolloidal structures with tailored surface chemistry can potentially be created by adsorbing different types of colloidal particles onto the outer shell.<sup>6</sup> The concepts shown here can potentially also be extended to bulk emulsification techniques for the preparation of nonspherical structures in larger quantities, albeit with a poorer control over the droplet size and monodispersity.



This new approach is thus a promising route toward the controlled fabrication of anisotropic supracolloidal structures with deliberately designed shapes and surface chemistry.

## Conclusions

Nonspherical supracolloidal structures with well-defined shapes were fabricated through the arrested coalescence of monodisperse droplets partially coated with colloidal particles. Droplet coalescence was arrested due to the jamming of colloidal particles at the oil–water interface before complete fusion of droplets. Jamming occurs because of the increase in particle coverage on the droplet surface as the droplet surface-to-volume ratio increases during the fusion process. The ability of jammed particles to withstand unequal stresses along the oil–water interface allows the formation of stable structures with a variety of anisotropic shapes. We show that, by adjusting the initial surface coverage by particles, more than two droplets can coalesce to form multiunit structures. The shape of these multiunit structures can be tuned by assembling the single droplets into predefined arrays before the onset of coalescence. As an example, multiunit structures with bonding angles of 60 and 120° were produced by arranging droplets into hexagonal arrays at an air–water interface prior to coalescence. The possibility to precisely control the droplet size and to deliver colloidal particles in a controllable fashion to the droplet surface makes microfluidic devices a powerful tool for the generation of structures with anisotropic shape. Nonspherical supracolloidal structures produced with this approach can be exploited as anisotropic building blocks for the fabrication of novel complex materials.

**Acknowledgment.** This work was supported by BASF, the NSF (DMR-0602684), the Harvard MRSEC (DMR-0820484), and the Swiss National Science Foundation (PBSK2-116386/1).

**Supporting Information Available:** A movie is available to illustrate the arrested coalescence of 100  $\mu\text{m}$  droplets partially coated with CTAB-modified silica particles. The sequence of images was acquired using a fast camera coupled to an optical microscope at a speed of 20 000 frames/second. The movie shown was slowed by a factor of 2000. This material is available free of charge via the Internet at <http://pubs.acs.org>.

## References and Notes

- (1) Utada, A. S.; Lorenceau, E.; Link, D. R.; Kaplan, P. D.; Stone, H. A.; Weitz, D. A. *Science* **2005**, *308* (5721), 537–541.
- (2) Leunissen, M. E.; Christova, C. G.; Hynninen, A. P.; Royall, C. P.; Campbell, A. I.; Imhof, A.; Dijkstra, M.; van Roij, R.; van Blaaderen, A. *Nature* **2005**, *437* (7056), 235–240.
- (3) Kim, S. H.; Heo, C. J.; Lee, S. Y.; Yi, G. R.; Yang, S. M. *Chem. Mater.* **2007**, *19* (19), 4751–4760.
- (4) Dinsmore, A. D.; Hsu, M. F.; Nikolaides, M. G.; Marquez, M.; Bausch, A. R.; Weitz, D. A. *Science* **2002**, *298* (5595), 1006–1009.
- (5) Velev, O. D.; Furusawa, K.; Nagayama, K. *Langmuir* **1996**, *12* (10), 2374–2384.
- (6) Subramaniam, A. B.; Abkarian, M.; Stone, H. A. *Nat. Mater.* **2005**, *4* (7), 553–556.
- (7) Binks, B. P.; Horozov, T. S. *Colloidal Particles at Liquid Interfaces*; Cambridge University Press: Cambridge, U.K., 2006; p 518.
- (8) Gonzenbach, U. T.; Studart, A. R.; Tervoort, E.; Gauckler, L. J. *Angew. Chem., Int. Ed.* **2006**, *45* (21), 3526–3530.
- (9) Subramaniam, A. B.; Abkarian, M.; Mahadevan, L.; Stone, H. A. *Nature* **2005**, *438* (7070), 930–930.
- (10) Bon, S. A. F.; Mookhoek, S. D.; Colver, P. J.; Fischer, H. R.; van der Zwaag, S. *Eur. Polym. J.* **2007**, *43* (11), 4839–4842.
- (11) Kim, J. W.; Lee, D.; Shum, H. C.; Weitz, D. A. *Adv. Mater.* **2008**, *20*, 3239–3243.
- (12) Studart, A. R.; Gonzenbach, U. T.; Akartuna, I.; Tervoort, E.; Gauckler, L. J. *J. Mater. Chem.* **2007**, *17* (31), 3283–3289.
- (13) Atkin, R.; Craig, V. S. J.; Biggs, S. *Langmuir* **2000**, *16* (24), 9374–9380.
- (14) Lianos, P.; Zana, R. *J. Colloid Interface Sci.* **1981**, *84* (1), 100–107.
- (15) Fuerstenau, D. W. *J. Phys. Chem.* **1956**, *60* (7), 981–985.

JP806795C